STARS

University of Central Florida
STARS

Faculty Bibliography 2010s

Faculty Bibliography

1-1-2011

Simultaneous ranging and velocimetry of fast moving targets using oppositely chirped pulses from a mode-locked laser

Mohammad U. Piracha
University of Central Florida

Dat Nguyen
University of Central Florida

Ibrahim Ozdur
University of Central Florida

Peter J. Delfyett
University of Central Florida

Find similar works at: https://stars.library.ucf.edu/facultybib2010

University of Central Florida Libraries http://library.ucf.edu

Recommended Citation

University of Central Florida

STARS
Showcase of Text, Archives, Research & Scholarship

Simultaneous ranging and velocimetry of fast moving targets using oppositely chirped pulses from a mode-locked laser

Mohammad U. Piracha,[1,2] Dat Nguyen,[1] Ibrahim Ozdur,[1] and Peter J Delfyett[1,3]

[1]CREOL, The College of Optics and Photonics, University of Central Florida, Orlando, Florida 32816, USA
[2]mpiracha@creol.ucf.edu
[3]delfyett@creol.ucf.edu

A lidar system based on the coherent detection of oppositely chirped pulses generated using a 20 MHz mode locked laser and chirped fiber Bragg gratings is presented. Sub millimeter resolution ranging is performed with > 25 dB signal to noise ratio. Simultaneous, range and Doppler velocity measurements are experimentally demonstrated using a target moving at > 330 km/h inside the laboratory.

OCIS codes: (280.3640) Lidar; (280.3340) Laser Doppler velocimetry (140.4050) Mode-locked lasers; (120.0120) Instrumentation, measurement, and metrology; (280.0280) Remote sensing and sensors.

References and links

1. T. Fujii, and T. Fukuchi, *Laser Remote Sensing* (Taylor & Francis, 2005).
2. M. I. Skolnik, *Introduction to Radar Systems* (McGraw-Hill, 2001).
3. H. Araki, S. Tazawa, H. Noda, Y. Ishihara, S. Goossens, S. Sasaki, N. Kawano, I. Kamiya, H. Otake, J. Oberst, and C. Shum, "Lunar global shape and polar topography derived from Kaguya-LALT laser altimetry," Science **323**(5916), 897–900 (2009).
4. "Lidar Tracks CO_2," Gary Gimmestad, SPIE Professional January, 2011.
5. B. W. Schilling, D. N. Barr, G. C. Templeton, L. J. Mizerka, and C. W. Trussell, "Multiple-return laser radar for three-dimensional imaging through obscurations," Appl. Opt. **41**(15), 2791–2799 (2002).
6. M.-C. Amann, T. Bosch, M. Lescure, R. Myllylä, and M. Rioux, "Laser ranging: a critical review of usual techniques for distance measurement," Opt. Eng. **40**(1), 10 (2001).
7. R. Agishev, B. Gross, F. Moshary, A. Gilerson, and S. Ahmed, "Range-resolved pulsed and CWFM lidars: potential capabilities comparison," Appl. Phys. B **85**(1), 149–162 (2006).
8. X. Sun, J. B. Abshire, M. A. Krainak, and W. B. Hasselbrack, "Photon counting pseudorandom noise code laser altimeters," Proc. SPIE **6771**, 677100 (2007).
9. P. A. Hiskett, C. S. Parry, A. McCarthy, and G. S. Buller, "A photon-counting time-of-flight ranging technique developed for the avoidance of range ambiguity at gigahertz clock rates," Opt. Express **16**(18), 13685–13698 (2008).
10. J. Lee, Y.-J. Kim, K. Lee, S. Lee, and S. Kim, "Time-of-flight measurement with femtosecond light pulses," Nat. Photonics **4**(10), 716–720 (2010).
11. I. Coddington, W. C. Swann, L. Nenadovic, and N. R. Newbury, "Rapid and precise absolute distance measurements at long range," Nat. Photonics **3**(6), 351–356 (2009).
12. Z. W. Barber, W. R. Babbitt, B. Kaylor, R. R. Reibel, and P. A. Roos, "Accuracy of active chirp linearization for broadband frequency modulated continuous wave ladar," Appl. Opt. **49**(2), 213–219 (2010).
13. K. W. Holman, D. G. Kocher, and S. Kaushik, "MIT/LL development of broadband linear frequency chirp for high-resolution ladar," Proc. SPIE **6572**, 65720J (2007).
14. N. Satyan, A. Vasilyev, G. Rakuljic, V. Leyva, and A. Yariv, "Precise control of broadband frequency chirps using optoelectronic feedback," Opt. Express **17**(18), 15991–15999 (2009).
15. A. Vasilyev, N. Satyan, S. Xu, G. Rakuljic, and A. Yariv, "Multiple source frequency-modulated continuous-wave optical reflectometry: theory and experiment," Appl. Opt. **49**(10), 1932–1937 (2010).
16. P. A. Roos, R. R. Reibel, T. Berg, B. Kaylor, Z. W. Barber, and W. R. Babbitt, "Ultrabroadband optical chirp linearization for precision metrology applications," Opt. Lett. **34**(23), 3692–3694 (2009).
17. S. M. Beck, J. R. Buck, W. F. Buell, R. P. Dickinson, D. A. Kozlowski, N. J. Marechal, and T. J. Wright, "Synthetic-aperture imaging laser radar: laboratory demonstration and signal processing," Appl. Opt. **44**(35), 7621–7629 (2005).

18. C. J. Karlsson, F. A. A. Olsson, D. Letalick, and M. Harris, "All-fiber multifunction continuous-wave coherent laser radar at 1.55μm for range, speed, vibration, and wind measurements," Appl. Opt. **39**(21), 3716–3726 (2000).
19. R. Schneider, P. Thurmel, and M. Stockmann, "Distance measurement of moving objects by frequency modulated laser radar," Opt. Eng. **40**(1), 33–37 (2001).
20. D. F. Pierrottet, F. Amzajerdian, L. Petway, B. Barnes, G. Lockard, and M. Rubio, "Linear FMCW laser radar for precision range and vector velocity measurements," Proc. Mater. Res. Soc. Symp. (2008).
21. R. E. Saperstein, N. Alic, S. Zamek, K. Ikeda, B. Slutsky, and Y. Fainman, "Processing advantages of linear chirped fiber Bragg gratings in the time domain realization of optical frequency-domain reflectometry," Opt. Express **15**(23), 15464–15479 (2007).
22. K. Kim, S. Lee, and P. J. Delfyett, "eXtreme chirped pulse amplification beyond the fundamental energy storage limit of semiconductor optical amplifiers," IEEE J. Sel. Top. Quantum Electron. **12**(2), 245–254 (2006).
23. S. Lee, D. Mandridis, and P. J. Delfyett, Jr., "eXtreme chirped pulse oscillator operating in the nanosecond stretched pulse regime," Opt. Express **16**(7), 4766–4773 (2008).
24. M. U. Piracha, D. Nguyen, D. Mandridis, T. Yilmaz, I. Ozdur, S. Ozharar, and P. J. Delfyett, "Range resolved lidar for long distance ranging with sub-millimeter resolution," Opt. Express **18**(7), 7184–7189 (2010).
25. J. A. Conway, G. A. Sefler, J. T. Chou, and G. C. Valley, "Phase ripple correction: theory and application," Opt. Lett. **33**(10), 1108–1110 (2008).
26. T.-J. Ahn, J. Y. Lee, and D. Y. Kim, "Suppression of nonlinear frequency sweep in an optical frequency-domain reflectometer by use of Hilbert transformation," Appl. Opt. **44**(35), 7630–7634 (2005).

1. Introduction

Lidar systems are important for performing many different tasks such as remote sensing, altimetry and imaging [1–5]. Frequency modulated continuous wave (FMCW) and Time of flight (TOF) are two common types of lidar systems [6,7]. For unambiguous long distance measurements with TOF lidar systems, low pulse repetition frequencies (PRF) must be used to prevent aliasing. One way to overcome this limit is to modulate the laser with pseudorandom noise codes [8,9]. Recently, Joohyung et al. achieved time of flight precision in the nanometer regime by phase locking the pulse repetition rate using optical cross correlation [10]. High resolution absolute distance measurements were demonstrated by Codington et al. using a novel multi-heterodyne approach using optical frequency combs [11]. Conventional TOF lidars require short pulses of less than 6.7 ps duration for submillimeter resolution. Unfortunately with such short pulses, the damage threshold of optical amplifiers and nonlinear effects imposes a limit on the peak pulse power and thus, the maximum ranging distance.

Frequency modulated continuous wave (FMCW) lidars rely on linearly ramping the optical frequency of a laser and interfering the delayed echo signal with a reference signal to produce a beat signal. The frequency of the beat signal corresponds to the target distance [6]. The performance of FMCW lidars is affected by the span, duration, and linearity of the optical frequency sweep [12]. Optical frequency sweeps of several GHz have been reported [13, 14]. For sub-millimeter resolution, optical bandwidths of hundreds of GHz are required. An algorithmic stitching approach was used in [15] to increase the effective bandwidth of a FMCW system resulting in 500 μm range resolution. A frequency chirp bandwidth of almost 5 THz was also demonstrated using a self-heterodyne technique [16]. The maximum range of a FMCW lidar system is limited by the coherence length of the laser source. Beck et al. demonstrated a synthetic aperture laser radar employing a tunable laser with ~1 km coherence length, and a digital reference channel signal was used to correct for phase errors [17].

In most laser ranging systems, it is possible to determine the velocity of a target by recording the change in target distance with time. However, the FMCW technique offers the advantage of direct velocity measurements. This is done by using optical waveforms with triangular waveform frequency modulation (i.e. periodic, opposite frequency chirps) that result in the generation of Doppler beat signals that can be directly measured [18–20].

In this paper, a lidar system that combines the benefits of the FMCW and TOF techniques is presented. Our lidar concept is based on the generation of temporally stretched, frequency chirped pulses from a mode locked laser using a chirped fiber Bragg grating (CFBG) [21]. Unlike TOF systems, the range resolution is not defined by the width of the laser pulses and

sub-millimeter resolution is obtained using pulses that are a few meters long. A signal to noise ratio (SNR) of > 25 dB is achieved. A high PRF of 20 MHz provides fast update rates. In addition to this, our lidar design allows easy amplification of optical signals to high power levels for long distance ranging using the extremely stretched pulse amplification (XCPA) technique [22,23], while minimizing fiber non-linearities. The narrow optical linewidth of the mode locked laser results in optical pulses with coherence lengths of tens of kilometers that enable long distance operation with coherent detection at the receiver. Recently, a pulse tagging scheme based on phase modulation to perform unambiguous long distance measurements was demonstrated using temporally stretched, frequency chirped pulses [24]. Here, we utilize a train of oppositely chirped pulses to probe a fast moving target that results in the generation of a Doppler shifted beat signal that provides range and velocity measurements simultaneously while benefitting from the advantages offered by the temporally stretched, frequency chirped pulse lidar approach. Moreover, this is to the best of our knowledge, the first experimental demonstration of velocimetry with a target moving at speeds of over 330 km/h inside a laboratory. Simulations are performed to confirm the effect of the non-ideal behavior of the chirped fiber Bragg grating on lidar performance and a close agreement between experiment and theory is observed.

2. Temporally stretched, frequency chirped lidar for simultaneous velocity and range measurements

2.1 Interference of oppositely chirped pulses

The interference of oppositely chirped pulses is shown in Fig. 1(a). One pulse train (echo signal) is Doppler shifted in frequency and is also delayed in time relative to the reference pulse train. This results in the generation of a beat tone at frequency f_{up} in the up-chirped pulses, and another beat tone at frequency f_{down} in the down-chirped pulses as shown in Fig. 1(b). The dispersion (D = 1651 ps/nm) of the CFBG can be expressed in terms of a chirp parameter S that is obtained by converting the dispersion units (from temporal delay per unit wavelength), to distance per unit optical frequency and then taking its inverse. This yields S = 250 MHz/mm, which implies a shift of 250 MHz in beat frequency for a 1 mm change in the target round trip distance. The one way target distance (d) is calculated by $d = f_{center} / 2S$ where $f_{center} = (f_{up} + f_{down}) / 2$. The velocity is given by $v = \Delta f \cdot \lambda / 4$ where $\Delta f = f_{down} - f_{up}$, and λ is the center wavelength. Since the observed frequency difference Δf is twice the actual Doppler shift in the echo signal, a factor of 2 has been included in the velocity calculation to account for this [2]. If $f_{down} > f_{up}$, the target is moving towards the observer, and vice versa.
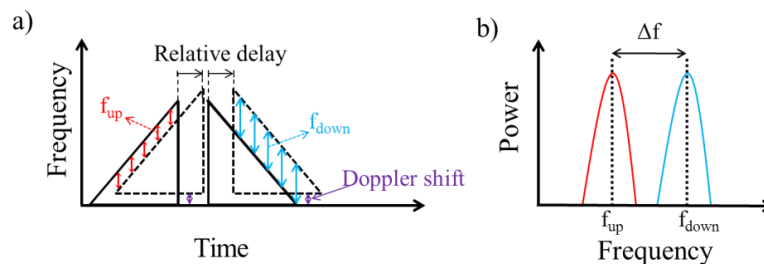

Fig. 1. (a) The interference of oppositely chirped pulse trains. One pulse train is Doppler shifted and temporally delayed with respect to the other (b) This results in the generation of a beat signal that contains decoupled distance and velocity information.

2.2 Experimental setup for simultaneous, decoupled velocity and distance measurements

The lidar setup consists of two parts. The first part generates a train of oppositely chirped pulses as shown in Fig. 2(a). A commercially available passively mode locked laser with a pulse repetition frequency (PRF) of 20 MHz and a center wavelength of 1548 nm is used to

generate pulses with a full width at half maximum (FWHM) duration of < 1 ps corresponding to an optical bandwidth of ~750 GHz. On the other hand, the optical linewidth of a single axial mode component of the MLL is < 3 kHz enabling coherent lidar operation at distances of several tens of kilometers. The laser output is split in two arms, each with a polarization controller (PC), circulator and CFBG with a dispersion (D) of 1651 ps/nm. The sign of dispersion of the two CFBGs is opposite. A fiber delay is introduced in the upper arm to interleave the up-chirped and down-chirped pulses in the time domain. Stretched pulses of ~10 ns duration with a −3 dB optical bandwidth of ~6 nm (~750 GHz), centered at λ = 1548 nm are observed, yielding a time bandwidth product of ~7500. An erbium doped fiber amplifier (EDFA) is used to amplify the pulses to an average power of 276 mW. Since the gain of the EDFA is not uniform across all wavelengths, the amplified pulses exhibit a stronger intensity at shorter wavelengths and this can be used to obtain the sign of the chirp (and the corresponding beat frequency).

The second part of the setup consists of a lidar interferometer as shown in Fig. 2(b). A directional coupler splits the pulse train into two arms. The target arm consists of a circulator that directs the pulses to a fiber launcher. The optical pulses are launched to a target located about 20 cm away.
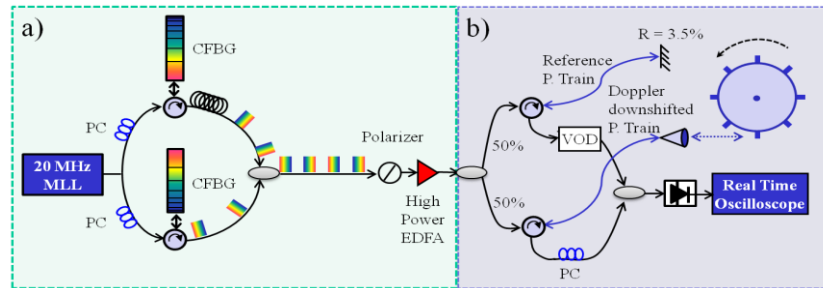

Fig. 2. Lidar schematic. (a) Setup for generation of temporally stretched, oppositely chirped pulses. (b) lidar interferometer setup. MLL, Mode Locked Laser; PC, Polarization Controller; CFBG, Chirped Fiber Bragg Grating; P. Train, Pulse Train; VOD, Variable Optical Delay; EDFA, Erbium Doped Fiber Amplifier.

The target consists of a 1 mm thick plastic disc with a radius of 6 cm. Its outer surface is machined to form small teeth that are covered with retro-reflecting tape to ensure easy collection of the echo signal without the need for careful optical alignment. The disc is mounted on a Dremel rotary tool and can be spun at thousands of revolutions per minute. The Dremel tool and disc are placed inside a metal enclosure due to safety considerations.

In the target arm, the optical signal is launched to probe a single tooth on a stationary plastic disc. The echo signal travels back to the circulator, and is directed to a directional coupler after passing through a PC. The PC is used to match the polarization of the lidar arms. The reference arm uses the reflection from the facet of the FC/PC fiber connector as the reference signal. The VOD is tuned and the stationary disc is manually rotated to adjust the position of the teeth such that the optical path lengths of lidar interferometer arms are equal (i.e. beat tone is centered at DC) when the laser beam probes a single tooth at normal incidence. This position of the target is referred to as the mean target position in the remainder of this paper.

After the Dremel tool is switched on to spin the disc, an average echo signal power of 22.5 μW is observed at the input of the directional coupler. The average reference signal power is 0.75 mW. For simultaneous velocity and distance measurements, the disc is spun at thousands of revolutions per minute resulting in an echo signal that is Doppler down-shifted in frequency because the teeth on the disc are moving along the direction of the probing beam. A directional coupler directs the optical interference signal to a 15 GHz photodetector resulting in coherent detection. The photodetected waveform of 40 μs duration is acquired

using an 8 GHz real-time oscilloscope. A 1 µs time window is used to take Fourier transforms of different segments of the acquired pulse train to observe Doppler splitting to directly measure target velocity. The shift in the beat signals is also recorded to obtain distance and velocity information as a function of time (Fig. 3).
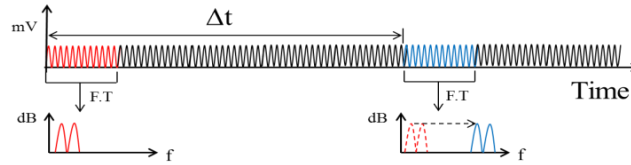

Fig. 3. A 1 µs time window is used to take Fourier transforms (F.T) of different segments of the acquired pulse train to observe beat tones that provide distance and velocity information.

2.3 Results

The Fourier transform of a 1 µs segment (from 12 – 13 µs) of the acquired pulse train reveals f_{center} = 1 GHz and Δf = 0.24 GHz as shown in Fig. 4(a). This corresponds to a target distance of d = f_{center} / 2D = 2 mm from the mean position and a velocity of v = $\Delta f . \lambda / 4$ = 94 m/s. A signal to noise ratio of at least 25 dB is observed. A similar analysis of another segment from 39 – 40 µs reveals that the beat frequencies have shifted and a new value of f_{center} = 2.28 GHz, corresponding to a new target distance of d = 4.56 mm (from the mean position) is observed. The width of each of the two notes is less than 140 MHz, resulting in a range resolution of < 0.3 mm. A beat note separation of Δf = 0.24 GHz is maintained, indicating a velocity of 94 m/s, which is in agreement with the previous velocity measurement. Separate Fourier transforms of the up and down-chirped pulses reveal $f_{down} > f_{up}$, indicating motion of the target away from the observer. The distance and velocity of the target at different times are given in Fig. 4(b). It must be noted that the beat notes in Fig. 4(a) are not single tones, but envelope structures over an array of narrow lines separated by 20 MHz (corresponding to the PRF of the MLL). For more accurate measurements, the 'center of mass' of the beat envelope can be determined or a MLL with a lower PRF can be used.

(a)

(b)

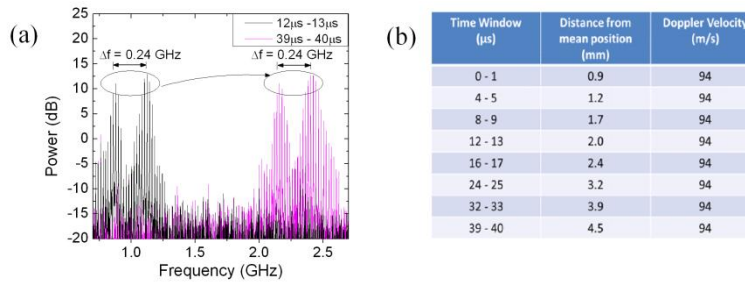| Time Window (µs)	Distance from mean position (mm)	Doppler Velocity (m/s)
0 - 1	0.9	94
4 - 5	1.2	94
8 - 9	1.7	94
12 - 13	2.0	94
16 - 17	2.4	94
24 - 25	3.2	94
32 - 33	3.9	94
39 - 40	4.5	94

Fig. 4. (a) The observed beat notes at different times (b) Target distance and velocity at different times.

The velocity of the target can also be obtained by calculating the distance travelled by the target over a finite time duration. In the data shown in Fig. 4(b), the target travels a total distance of 4.5 mm – 0.9 mm = 3.6 mm, over the entire duration of 39 µs, resulting in a velocity of 92 m/s in a direction away from the observer. This is in very close agreement with the target velocity calculated using the Doppler shift.

3. Discussion

The range resolution of the lidar is given by c/2B where c is the speed of light and B is the bandwidth of the lidar signal. With an optical bandwidth (B) of about ~750 GHz, a range resolution of ~200 µm should be theoretically possible. However, a resolution of < 300 µm is

observed at small relative pulse delays. This may be due to the group delay ripple (GDR) of the CFBGs, as shown in Fig. 5(a). Moreover, the CFBGs used in this setup have a dispersion that is linear with respect to wavelength. Therefore they generate stretched pulses that do not have a perfectly linear chirp in the optical frequency domain.

To confirm the effect of the GDR and the nonlinear optical frequency chirp of the CFBG, a simulation was performed using the dispersion profile of one of the CFBGs (as supplied by the manufacturer). A square shaped input optical spectrum from 1550 nm to 1556 nm was assumed and a pulse train with only up-chirped pulses was considered. The results obtained for different simulated target distances are given in Fig. 5(b). It is evident that the beat signal width increases as the relative difference between the interfering pulses increases.
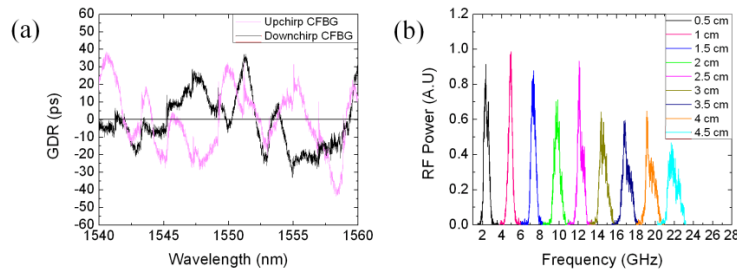

Fig. 5. (a) GDR of the two CFBGs (b) Simulation results at different target distances confirm the broadening of the RF beat tones.

In the lidar system presented, two CFBGs, each with a dispersion of 1651 ps/nm are used. However, the GDR profiles of the two gratings are different as can be seen in Fig. 5(a). Due to this, the shapes of the Doppler shifted beat notes (f_{up} and f_{down}) do not look identical, as evident in Fig. 4(a). The setup can be modified as in [21] to achieve Doppler shifted beat notes with identical widths and profiles.

Since the chirped pulses (of 10 ns duration) do not completely cover the pulse period, the PRF of the MLL can be tuned by ~10 kHz to shift the relative position between two pulse trains by 50 ns at a range of ~10 km. Moreover, a MLL with a higher PRF, a CFBG with higher dispersion, or a MLL with a larger optical bandwidth can also be used to completely fill the time slots of the pulse train to ensure pulse overlap at all times.

When moving targets are probed with the lidar, the beat signal frequency continuously shifts over the duration of the 1 μs observation time window that is used for taking Fourier transforms. In our experiment, the motion of the target results in the broadening of the width of each beat tone by 47 MHz. This reduces the range resolution of the system and also imposes a limit on the smallest target velocity that can be measured. If the full width at half maximum (FWHM) of each Doppler shifted tone is 140 MHz, then the minimum resolvable velocity (−3 dB down) is ~54 m/s. This limitation does not apply for velocity measurements that are made by calculating the displacement of the target over small time durations, as discussed in section 2.3. It may be possible to reduce the broadening due to GDR by using an approach similar to [25, 26].

4. Conclusion

An oppositely chirped pulse lidar with a pulse repetition frequency of 20 MHz using a mode locked laser is presented. Range measurements of a moving target are demonstrated in the laboratory with sub-millimeter resolution and simultaneous, decoupled Doppler velocity measurements are performed using a target moving at a velocity of ~92 m/s (331 km/h). The direction of the target is also directly calculated from the received signal. The velocity measurements are further verified by tracking the target position with respect to time. Coherent detection at the receiver results in an SNR of > 25 dB. Furthermore, simulations are

performed to confirm the effect of the non-ideal behavior of the chirped fiber Bragg grating and a good agreement between the theoretical and experimentally observed lidar performance is observed.